Journal of Inorganic and General Chemistry
ZAAC
Zeitschrift für anorganische und allgemeine Chemie

DOI: 10.1002/zaac.201700088

ARTICLE

Synergistic Catalytic Effect of a Series of Energetic Coordination Compounds based on Tetrazole-1-acetic Acid on Thermal Decomposition of HMX

Yuan-Yuan Qu,[a] Zhi-Xian Wei,*[b] Li Kang,[a] Fei Xie,[a] He-Dan Zhang,[b] and Pan Yue[b]

Abstract. A series of energetic coordination compounds $[Co(tza)_2]_n$ (**1**), $[Bi(tza)_3]_n$ (**2**), $\{[Cu_4(tza)_6(OH)_2]\cdot 4H_2O\}_n$ (**3**), $[Mn(tza)_2]_n$ (**4**), $\{[Bi(tza)(C_2O_4)(H_2O)]\cdot H_2O\}_n$ (**5**) and $[Fe_3O(tza)_6(H_2O)_3]NO_3$ (**6**) based on tetrazole-1-acetic acid (Htza) were synthesized though environmentally friendly methods. The coordination compounds were characterized by elemental analyses, IR spectroscopy, single-crystal and powder X-ray diffraction (PXRD), thermogravimetric analyses (TG), and differential scanning calorimetry (DSC). Their catalytic performances and the synergetic catalytic effects between **1** and **2**, **3** and **4**, **5** and **6** on the thermal decomposition of octahydro-1,3,5,7-tetranitro-1,3,5,7-tetrazocine (HMX) were all investigated by DSC. The results revealed that compounds **1**–**6** are thermally stable energetic compounds and they all exhibit high catalytic action for HMX thermal decomposition. The catalytic effects of the compounds on HMX thermal decomposition are closely related to the oxides, which come from the decomposition of the compounds, but have no positive relationships with the heat releases of the compounds themselves. Moreover, the synergistic catalytic effects between **1** and **2**, **3** and **4**, **5** and **6** were observed. Their mixtures at different mass ratio have different synergetic catalytic effects, and the sequence of the biggest synergetic index (SI) in each system is copper-manganese system (compounds **3** and **4**) > iron-bismuth system (compounds **5** and **6**) > cobalt-bismuth system (compounds **1** and **2**), indicating that the synergistic catalytic effects are mainly related to the combination and the proportion of the compounds.

Introduction

Ammonium perchlorate (AP), cyclotrimethylene trinitramine (RDX), and cyclotetramethylene tetranitramine (HMX) are the main ingredients in solid propellants, and hence their thermal decomposition characteristics directly influence the combustion performance of the solid propellants.[1–4] Energetic coordination compounds used as the catalysts/additives to the propellants have attracted tremendous interests for such compounds not only contain more N=N or C=N groups, which hold a higher positive enthalpy formation but also provide fresh metal or metal oxide at the molecule level on the propellant surface, which could improve combustion performance when the compounds are used as the catalysts/additives to the propellants.[5] Hence, a lot of energetic metal compounds have been researched recently as catalysts for the thermal decomposition of AP, RDX, and HMX, such as a series of ferrocenyl compounds,[6–10] two energetic complexes, $Co(TO)_2(DNBA)_2(H_2O)_2$ and Cu(TZA)(DNBA), incorporating 3,5-dinitrobenzoic acid and azole ligands,[11] $[Mn(BTO)(H_2O)_2]_n$ [BTO = 1H,1′H-[5,5′-bitetrazole]-1,1′-bis(olate)].[12] Among those energetic metal compounds, most of them show excellent catalytic activities for AP and RDX thermal decomposition, however, rare have distinct catalytic effects on the thermal decomposition of HMX [the oxidizer in nitrate ester plasticized polyether (NEPE) solid propellant]. Hence, it is worthwhile to investigate the high efficient catalysts for HMX thermal decomposition, and one can choose excellent combustion catalysts for NEPE propellant further.

Single metal compounds always show limit catalytic effects for the complex propellant components in most cases, and mixed/compositive/polynuclear metal energetic compounds as combustion catalysts should be researched and chose.[13–15] The mixed/compositive/polynuclear metal energetic compounds can produce multiple or more metal or metal oxide mixtures on the propellants surface than single metal compounds at the molecule level and then can offer a wider range of selective or synergetic catalytic effects.[16] Therefore, using the synergies between different metal compounds to improve the combustion properties of solid propellants should be studied as an important issue. But, to our best knowledge, rarely studies in this part have been reported so far.

Tetrazole-1-acetic (Htza), an important energetic ligand, has been widely used in the synthesis of energetic compounds such as $[Pb(tza)_2]_n$,[17] $[Bi(tza)_3]_n$,[18] $\{[Fe^{II}Fe^{III}{}_3O(tza)_6(H_2O)_3]\cdot 3NO_3\cdot 5H_2O\}_n$,[19] $[M(tza)_2]$ (M = Zn, Cd, Mn),[20] and a series of Cu^{II} coordination compounds.[21] However, their catalytic effect on the thermal decomposition of HMX have not been studied so far. As environmental friendly metal ions, the oxides or compounds of bismuth, manganese, iron, and copper, such as Bi_2WO_6,[15] $[Mn(BTA)(phen)_2\cdot 5H_2O]_n$,[22] Cu(Hatrz)(pda)$(H_2O)\cdot H_2O$, Cu^ICu^{II}(atrz)(pda)(H_2O)[23] and some ferrocenyl compounds,[10] have been synthesized and used to catalyze the

---

* Dr. Z.-X. Wei
E-Mail: zx_wei@126.com
[a] Department of Chemistry
School of Science
3 Xueyuan Road
Taiyuan, Shanxi, 030051, P. R. China
[b] Department of Safety Science and Engineering
Chemical Engineering and Environment Institute
3 Xueyuan Road
Taiyuan, Shanxi, 030051, P. R. China

thermal decomposition of HMX and most of them exhibit good catalytic effects.

Considering the above research and the environmental protection, a series of environmental friendly energetic compounds based on Htza were synthesized though environmentally friendly methods and their catalytic effects on HMX thermal decomposition were all investigated. The compounds $[Co(tza)_2]_n$ (**1**) and $[Bi(tza)_3]_n$ (**2**) were obtained successively in one pot, when $Co(NO_3)_2$ and $Bi(NO_3)_3$ were added to the solution of Htza in order to obtain heteronuclear compounds. Compounds $\{[Bi(tza)(C_2O_4)(H_2O)]\cdot H_2O\}_n$ (**5**) and $[Fe_3O(tza)_6(H_2O)_3]NO_3$ (**6**) were also continuously synthesized in the similar way except that the reactants were different substances. Herein, it is noted that the compounds $\{[Cu_4(tza)_6(OH)_2]\cdot 4H_2O\}_n$ (**3**) and $[Mn(tza)_2]_n$ (**4**) could not be obtained in the similar way as described above, hence, they were synthesized separately and constituted a catalytic system in order to study their synergistic catalytic activity. In a word, the compounds **1** and **2**, **3** and **4**, **5** and **6** were divided into three different synergistic catalytic systems, respectively. Their synergistic catalytic effects on the thermal decomposition of HMX were also studied in this paper. The results would provide the basic data for finding the most efficient combustion catalysts for NEPE propellant.

Results and Discussion

Description of Methods for the Synthesis of Compounds 1–6

The structures of compounds **1** and **2** have been shown in detail by *Dong*[20] and *Wang*,[18] respectively. However, in this study, compounds **1** and **2** were synthesized successively by one-pot synthesis though an environmentally friendly method. That is different from that compound **1** was synthesized in a MeOH solution at room temperature by *Dong*[20] and compound **2** was synthesized in water under heating condition by *Wang*.[18] The structure of compound **3** has been reported by *Yu*,[21] which was synthesized at 80 °C and the pH value was 5.0. In this study, it was synthesized in water at room temperature, which is an more environmentally friendly method than that in the reference.[21] Compound **4** has an isomorphic framework with compound **1**, and has been synthesized by *Dong*[20] using the same method as for **1**. In this study, compound **4** was prepared in an ethanol aqueous solution. This method is more safer than using methanol solvent in the reference.[2] Compounds **5** and **6** were synthesized successively at 80 °C in aqueous solution by one-pot method in the previous work by our research group.[16] That is a simple efficient and eco-friendly aqueous solution method.

PXRD Analysis

PXRD patterns of compounds **1–6** were investigated in the solid state at room temperature (Figure 1). The experimental results are in good agreement with the simulated data based on the single-crystal structure analysis, indicating that the coordination compound structures are solved accurately and the products are single phase.

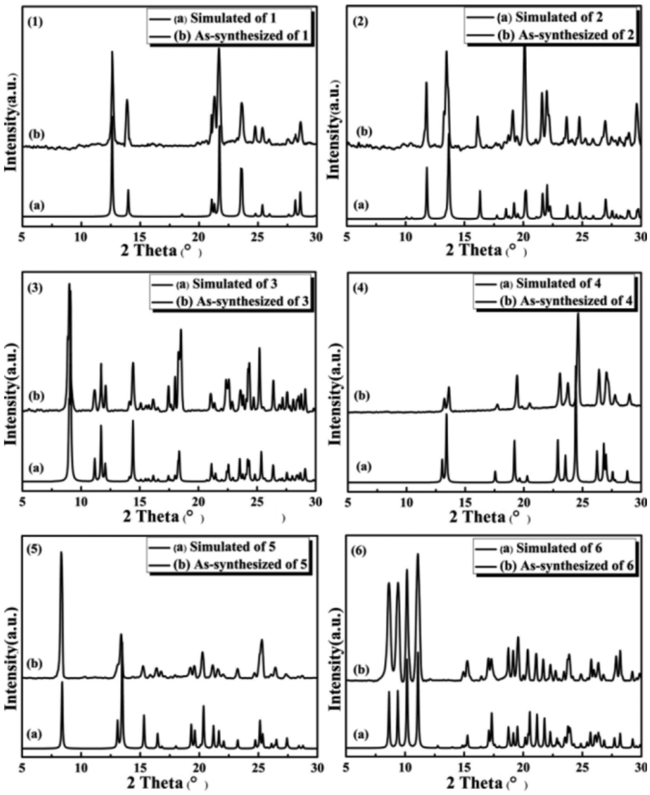

Figure 1. Experimental and simulated powder XRD patterns of compounds **1–6**.

Thermal Decomposition of Compounds 1–6

Thermal stability is an essential parameter for energetic compounds, because a higher thermal stability of an energetic coordination catalyst could add the steady of the solid propellant.[24] The thermal decomposition behaviors of the compounds above were investigated by TG-DSC. For compound **1** [Figure 2(1)], there is only one exothermic peak, which starts at 233.3 °C and ends at 340.2 °C in the DSC curve with the peak at a temperature of 291.5 °C, which represents the main decomposition process of the framework. The heat release of compound **1** is 1050.2 $J\cdot g^{-1}$. The corresponding TG curve of compound **1** shows that **1** undergoes a continuous weight-loss process from 197.5 to 539.2 °C, which is caused by the framework structure decomposition, producing some small solid and gas intermediate products with a lot of heat release in that stage. As the temperature increases, these intermediates are further decomposed and accompanied by a weak mass loss process. Finally, compound **1** completely converts to CoO with a residue weight percentage of 24.8 %, which is closed to the calculated value 24.0 %.

The exothermic peak of compound **2** [Figure 2(2)] starts at 224.2 °C and ends at 330.9 °C with the peak at a temperature of 252.9 °C, and the heat release of the decomposition process of compound **2** is 1146.4 $J\cdot g^{-1}$. There are two weight-loss stages in the TG curve of **2**, and the remaining weight corresponds to Bi_2O_3 with a residual amount of 37.9 % (calcd. 39.0 %).

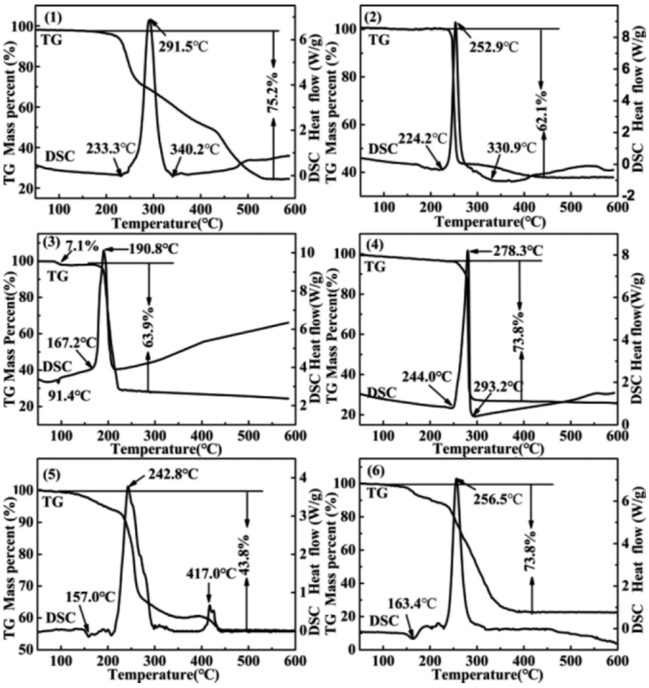

Figure 2. TG-DSC curves of compound **1**–**6**.

TG data for compound **3** [Figure 2(3)] show the initial weight loss step between 90.2 and 99.5 °C. The weight loss in this temperature range is about 7.1 %, corresponding to the loss of all water molecules (calcd. 6.4 %). The second obviously weight loss above 167.2 °C corresponds to the decomposition of the organic ligands. This weight loss process is identical to the exothermic peak that appeared on the DSC curve at 190.8 °C with a heat release of 732.4 $J\cdot g^{-1}$. The remaining weight corresponds to the CuO with residual amount of 29.0 %. That is close to the calculated value of 28.5 %.

For compound **4** [Figure 2(4)], there is only one exothermic process from 244.0 to 293.2 °C, with the peak at a temperature of 278.3 °C. This exothermic process represents the main decomposition reaction of compound **4** and the heat release is 706.2 $J\cdot g^{-1}$. There is one weight-loss stage in the TG curve of **4**, which is considered to be caused by the collapse of framework structure. Finally, compound **4** completely converts to MnO_2, with a residue percentage of 26.2 %, which is basically consistent with the calculated value (28.1 %).

The thermal decomposition process of compounds **5** [Figure 2(5)] and **6** [Figure 2(6)] have been described and analyzed in detail in our previous paper.[21] The decomposition peak temperatures (T_{exo}) and the heat release (ΔH) of compounds **1**–**6** are given in Table 1. From the data in Table 1, one can see that compounds **1**–**6** all have high decomposition temperatures and high energy release, so one can conclude that all of them are thermally stable energetic compounds.

Catalytic Effects of Compounds on the Thermal Decomposition of HMX

The effects on the thermal decomposition of HMX are important indexes for catalysts to evaluate their combustion catalytic activity. The thermal decomposition performance of HMX can be improved by reduce the peak temperature and increase the released heat through adding catalysts or additives.[5] In this study, the catalytic activity of all the prepared samples were investigated by DSC measurement.

Table 1. The decomposition temperatures and the heat release of compounds **1**–**6**.

Compound	T_{exo} a) /°C	ΔH b) /$J\cdot g^{-1}$
1	291.5	1050.2
2	252.9	1146.4
3	190.8	732.4
4	278.3	706.2
5	242.8	1004.8
6	256.5	982.6

a) T_{exo} = decomposition peak temperatures of samples. b) ΔH = heat release of the samples' exothermic processes.

Figure 3 shows the DSC curves for pure HMX and HMX with compounds **1**–**6**, respectively. As shown in Figure 3(a), there are two endothermic peaks and one exothermic peak in the thermal decomposition of pure HMX. The first endothermic peak at approximately around 194.3 °C is attributed to the phase transformation of HMX, and the second endothermic peak at 278.2 °C is caused by the melting of HMX. The exothermic peak for the HMX decomposition process is at 282.6 °C with the exothermic process value of 1047.6 $J\cdot g^{-1}$, which agrees basically with the reported one.[23,25]

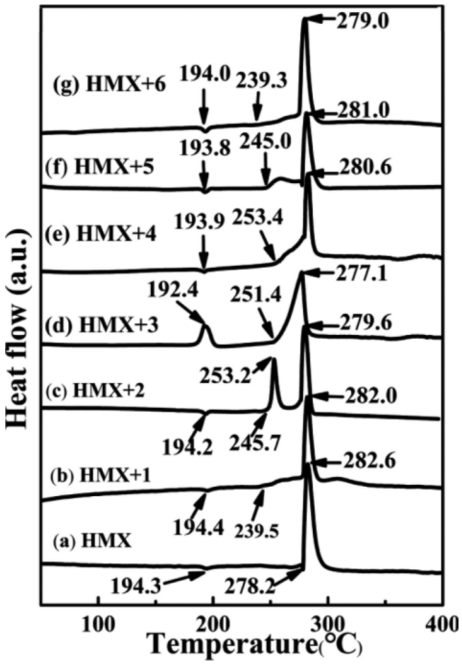

Figure 3. DSC curves of HMX and mixtures of HMX and compounds **1**–**6**, respectively.

Compared with the DSC curves of HMX in Figure 3, it is worth noting that there is no significant impact on the phase transition temperature of HMX with the addition of the compounds. The endothermic peak of the HMX melting process is incorporated into the exothermic peak, and the onset temperature of the exothermic peak is lower than that of the pure

HMX. The exothermic peak of HMX with compound **1** (curve b in Figure 3) starts at 239.5 °C and the decomposition peak temperature of HMX changes from 282.6 to 282.0 °C. The heat release of the exothermic process is 1333.1 $J \cdot g^{-1}$. The decomposition peak temperature of HMX with the addition of **2** (curve c) changes to 279.6 °C, and the heat release of the exothermic peak, which starts at 245.7 °C, is 1280.3 $J \cdot g^{-1}$. In curve d, there appears a small exothermic peak at 192.4 °C before the HMX exothermic peak, which is related to the framework structure collapse of **3**. This exothermic peak covers the HMX crystal transformation peak. The decomposition temperature of HMX advances to 277.1 °C, and the total heat release increases up to 1127.5 $J \cdot g^{-1}$. With the addition of compound **4** (curve e), the exothermic peak starts at 253.4 °C, and the decomposition temperature of HMX changes to 280.6 °C, with the heat release of 1145.4 $J \cdot g^{-1}$. The peak temperature of HMX containing compound **5** decreases to 281.0 °C and the heat release increases up to 1228.4 $J \cdot g^{-1}$, whereas these values for HMX containing **6** reaches 279.0 °C and 1291.4 $J \cdot g^{-1}$. The peak temperatures (T_{exo} in °C) of the HMX decomposition process and the heat release of the total heat release (ΔH in $J \cdot g^{-1}$) are listed in Table 2.

Table 2. Catalytic effects of compounds **1–6** on the thermal decomposition of HMX.

Sample	T_{exo} /°C	ΔH /$J \cdot g^{-1}$	$Q^{a)}$ /$J \cdot g^{-1}$	$\Delta T^{b)}$ /°C
HMX	282.6	–1047.6		
HMX+**1**	282.0	–1333.1	284.8	0.6
HMX+**2**	279.6	–1280.3	208.0	3.0
HMX+**3**	277.1	–1127.5	158.7	5.5
HMX+**4**	280.6	–1145.4	183.1	2.0
HMX+**5**	281.0	–1228.4	191.5	1.6
HMX+**6**	279.0	–1291.4	260.1	3.6

a) Q = measured value of the increased heat of the samples. b) ΔT = advanced decomposition peak temperature of HMX with addition of **1**–**6**.

Compared with the decomposition of pure HMX, the decomposition peak temperature advanced 0.6, 3.0, 5.5, 2.0, 1.6, and 3.6 °C and the heat release increased 284.8, 208.0, 158.7, 183.1, 191.5, and 260.1 $J \cdot g^{-1}$ through adding compounds **1–6**, respectively (Table 2). Herein, the values of the increased heat are obtained by subtracting the heat of the compounds and HMX itself. The decrease of the peak temperature and increase of the released heat indicating that compounds **1–6** have obviously catalytic effects on HMX thermal decomposition.

According to the decreased values of the HMX decomposition peak temperature, their catalytic efficiency in descending order is: **3** > **6** > **2** > **4** > **5** > **1**. However, considering the judgment criteria of the component compatibility of the propellants, the more the temperature decreases, the poorer the compatibility of the components is,[26] so we can not directly judge the qualities of the catalysts from the decreased values of the decomposition peak.

However, from the aspect of increasing the heat release, the catalytic abilities are **1** > **6** > **2** > **5** > **4** > **3**. This shows that compounds **1–6** have different catalytic effects on HMX thermal decomposition. During the thermal decomposition process, the mixtures not only release much heat themselves, but also generate corresponding metal oxides at a molecular level. Those metal oxides with different catalytic activity would not only change the decomposition mechanism of HMX but also catalyze further thermolysis of NO_x and the reactions among the products decompose from the HMX thermal decomposition and accelerate the decomposition of the corresponding condensed-phase products, increasing the heat release.[5] In addition, considering the heat release of the compounds themselves in Table 1, it can be seen that there are no positive relationships between the catalytic activity and the heat release of the energetic compounds themselves. For instance, the heat release of compound **3** is not much, but it makes the mixture system heat up the most, and it was the best catalyst among those energetic coordination compounds. Therefore, one can conclude that the catalytic effect of the compounds on HMX thermal decomposition could be closely related to the oxides, which come from the decomposition of the energetic compounds.

Synergetic Catalytic Effects of Coordination Compounds 1 and 2, 3 and 4, 5 and 6 on the Thermal Decomposition of HMX

HMX mixtures, which consisted of HMX and the mixtures of compounds, can produce multiple metal oxide in the decomposition process and then could offer a wider range of selective and synergetic catalytic effects. So the synergetic catalytic effects of the HMX mixtures on the thermal decomposition of HMX were also researched. Figure 4 shows the DSC curves

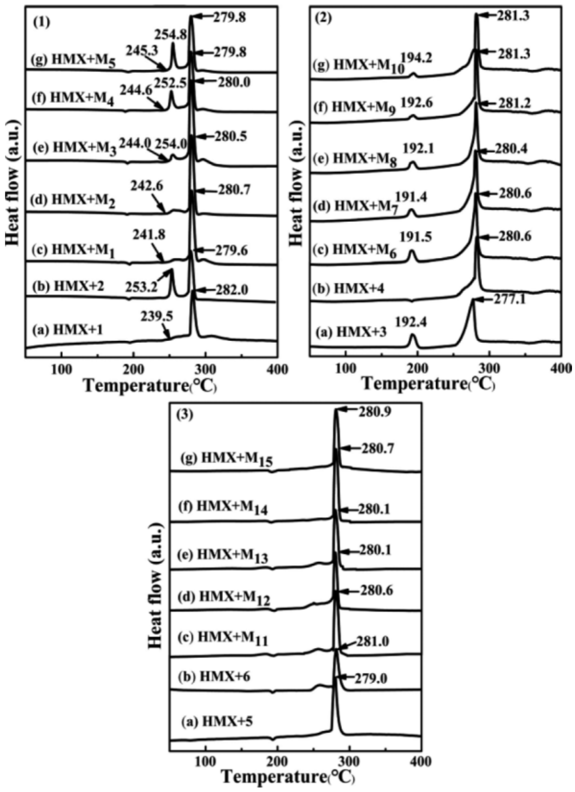

Figure 4. DSC curves of HMX with mixtures (1) M_1–M_5, (2) M_6–M_{10}, and (3) M_{11}–M_{15}.

of HMX mixtures. Since the shape of the DSC curves are similar (the differences are the temperatures of exothermic peaks and the heat release of the exothermic processes), the descriptions for DSC curves of HMX mixtures of compounds **1** and **2** were taken as examples. As shown in Figure 4(1), the DSC curves of HMX with different mass ratio mixtures of compounds **1** and **2** have some differences with that of HMX with **1** or **2**. Due to the addition of the mixtures of **1** and **2**, the decomposition peak temperatures of HMX change to 280.7, 280.5, 280.0, 279.8, and 279.8 °C. The heat release of the exothermic processes are 1322.9, 1355.5, 1451.8, 1369.9, and 1293.6 J·g^{-1}, respectively. Compared with pure HMX, the heat release of HMX with the mixtures increased by 268.3, 299.0, 391.3, 305.4, and 275.9 J·g^{-1}, respectively. All the data, including HMX with the mixtures of compounds **3** and **4**, **5** and **6**, are summarized in Table 3.

Table 3. The synergetic effect of compounds **1** and **2**, **3** and **4**, **5** and **6** in different mass ratios on the thermal decomposition of HMX.

Sample	T_{exo} /°C	ΔH /J·g^{-1}	Q /J·g^{-1}	Q_a $^{a)}$ /J·g^{-1}	SI$^{b)}$
HMX	282.6	–1047.6			
HMX+**1**	282.0	–1333.1	284.8		
HMX+**2**	279.6	–1280.3	208.0		
HMX+M_1	280.7	–1322.9	268.3	265.6	1.01
HMX+M_2	280.5	–1355.5	299.0	259.3	1.15
HMX+M_3	280.0	–1451.8	391.3	246.4	1.59
HMX+M_4	279.8	–1369.9	305.4	233.4	1.30
HMX+M_5	279.8	–1293.6	275.9	227.2	1.21
HMX+**3**	277.1	–1127.5	158.7		
HMX+**4**	280.6	–1145.4	183.1		
HMX+M_6	280.6	–1090.8	263.9	164.8	1.6
HMX+M_7	280.4	–1206.0	378.6	166.8	2.23
HMX+M_8	281.2	–1146.6	318.2	170.9	1.86
HMX+M_9	281.3	–1114.8	285.3	175.1	1.63
HMX+M_{10}	281.3	–1065.6	235.6	177.0	1.33
HMX+**5**	281.0	–1228.4	191.5		
HMX+**6**	279.0	–1291.4	260.1		
HMX+M_{11}	280.6	–1353.6	318.1	208.7	1.52
HMX+M_{12}	280.1	–1406.9	371.8	214.1	1.73
HMX+M_{13}	280.1	–1339.9	305.8	225.8	1.35
HMX+M_{14}	280.7	–1282.1	248.9	237.5	1.05
HMX+M_{15}	280.9	–1277.3	244.6	242.9	1.01

a) Q_a = arithmetic summation of the samples that compounds added alone. b) SI = synergetic index of compounds **1** and **2**, **3** and **4**, **5** and **6** in different mass ratios.

Compared with the addition of a single compound, the thermal decomposition peak temperature of HMX did not change much after adding the mixtures. But the heat releases of HMX mixtures are not a simple arithmetic summation of compounds added alone. The interaction between compounds **1** and **2**, **3** and **4**, **5** and **6** initiate the synergetic effects, which are considered responsible for the increased heat release.

We quantitatively evaluate the synergetic effect of the mixtures of compound **1** and **2** by using the synergetic index (SI) [Equation (1)]:[27]

$$SI = Q_m/(n_1Q_1 + n_2Q_2) \qquad (1)$$

where Q_1, Q_2, and Q_m are the increased heat release of HMX with the addition of **1**, **2**, and the mixtures of them, respectively, and the n_1 and n_2 are the mass fraction of **1** and **2** in the mixtures. The values of the SI are obtained to be 1.01, 1.15, 1.59, 1.30, and 1.21, respectively (Table 3). These results indicate that the co-existence of **1** and **2** show positive synergetic catalytic activity for the decomposition of HMX. When the mass ratio of **1** to **2** is 1:1, the system shows the best synergetic effect on the thermal decomposition of HMX. We use the same formula to calculate the SI between compounds **3** and **4**, **5** and **6** in different mass ratio, and the obtained values are listed in Table 3. When the mass ratio of **3** to **4** is 1:2, as well as **5** to **6** is 1:2, the systems show the best synergetic effect on the thermal decomposition of HMX, respectively.

As shown in Table 3 and Figure 4, three synergistic catalytic systems all show good synergistic effects, and the mixtures at different mass ratio have different synergetic catalytic effect on the HMX thermal decomposition, indicating that the SI in the same system are related to the proportion of the compounds. The sequence of the biggest synergetic index in each HMX mixture system is copper-manganese system (compounds **3** and **4**) > iron-bismuth system (compounds **5** and **6**) > cobalt-bismuth system (compounds **1** and **2**). Therefore, the synergistic catalytic effect is related to the compound composition of the system. In addition, the bismuth-cobalt system and the bismuth-iron system all have bismuth based compounds, and cobalt and iron both belong to iron-based elements. But the SI of bismuth-iron system is higher than that of bismuth-cobalt system, which may be due to the presence of iron in the compound **6** in a multinuclear fashion.

Conclusions

Compounds **1–6** are all thermally stable energetic compounds. They all have obviously different catalytic activity for the thermal decomposition of HMX. The catalytic effects of the compounds on HMX thermal decomposition are closely related to the oxides, which come from the decomposition of the compounds, but have no positive relationships with the heat release of the compounds themselves. The mixtures of compounds **1** and **2**, **3** and **4**, **5** and **6** can offer the synergistic catalytic for HMX thermal decomposition. The synergetic index (SI) of the copper-manganese system is higher than those of iron-bismuth and cobalt-bismuth system. The synergistic catalytic effects are mainly related to the combination and proportion of compounds in the systems.

Experimental Section

Materials and Methods: All chemicals used for the synthesis were obtained from commercial reagents of analytical grade and used without further purification. The elemental analyses data (C, H, and N) were carried out with a Vario ELIII elemental analyzer. Infrared (IR) spectra were performed from KBr pellets with a FTIR-8400S spectrometer photometer in the 4000–400 cm^{-1} region. XRD experiments for **1–6** were carried out with a Rigaku Mercury-CCD diffractometer with graphite-monochromated Mo-K_α radiation (λ = 0.71073 Å) at 293 K. The structures were solved by direct methods and anisotropically refined by least-squares on F^2 procedures using the SHELXTL-97. Powder X-ray diffraction (PXRD) intensities were measured at room temperature with a PANalytical X′Pert Pro diffractometer with Cu-K_α radiation. DSC-TG for compounds **1–6** were carried out with a Mettler Toledo DSC823E analyzer, and the samples were heated in a temperature range of 50–600 °C with a heating rate of 10 °C·min^{-1} in a flowing nitrogen atmosphere at 20 mL·min^{-1}. The DSC tests for HMX and HMX with additions were under the same condition with DSC-TG but heated in temperature range 50–400 °C and all samples were performed twice and the results were averaged.

Syntheses of $[Co(tza)_2]_n$ (1) and $[Bi(tza)_3]_n$ (2): A mixture of $Co(NO_3)_2$ (0.0582g, 0.2 mmol), $Bi(NO_3)_3$ (0.097g, 0.2 mmol), NH_2CH_2COOH (0.0225g, 0.3 mmol), and Htza (0.1024g, 0.8 mmol) were dissolved in ethanol (15 mL),. The mixture was transferred and sealed in a 25 mL Teflon-lined stainless-steel reactor and heated at 130 °C for 72 h. After slowly cooling to room temperature, pink rectangle crystals (compound **1**) were collected carefully from the wall of container. Afterwards, the white powder at the bottom of the container was filtered and washed with distilled water and ethanol several times, respectively. The white powders were redissolved in Htza solution (0.1 mol·L^{-1}, 10 mL), stirred at 90 °C for 1 h and filtered. The filtrate was placed at room temperature, and 10 d later, colorless block crystals were (compound **2**) obtained. Compound **1**: Yield 41 % (based on the Htza). $C_6H_6CoN_8O_4$ (313): calcd. C 23.00; H 1.92; N 35.78 %; found: C 22.91; H 1.91; N 35.63 %. **IR** (KBr): $\tilde{\nu}$ = 3174 s, 3032 w, 2947 w, 1624 s, 1489 w, 1434 m, 1402 s, 1318 m, 1183 m, 1103 m, 1005 m, 932 m, 890 w, 809 w, 702 m, 663 m cm^{-1}. Compound **2**: Yield 39 % (based on the Htza). $C_9H_9BiN_{12}O_6$ (590.26): calcd. C 18.30; H 1.52; N 28.46 %; found: C 18.02; H 1.59; N 28.66 %. **IR** (KBr): $\tilde{\nu}$ = 3174 s, 3139 w, 3089 w, 3000 w, 2948 w, 2359 s, 2337 s, 1602 s, 1574 s, 1488 w, 1426 m, 1395 s, 1180 m, 1103 m, 854 w, 792 w, 709 m cm^{-1}.

Synthesis of $\{[Cu_4(tza)_6(OH)_2]\cdot 4H_2O\}n$ (3): Htza (0.1537 g, 1.2 mmol) was dissolved in distilled water (12 mL), where NaOH (0.1 M) was added to adjust the pH at a value of 9.0. Afterwards $Cu(NO_3)_2\cdot 3H_2O$ (0.1450 g, 0.6 mmol) was added. The mixture was stirred at room temperature for 1 h. Two days later, blue block crystals were obtained. Yield: 45 % (based on Htza). $Cu_4C_{18}H_{28}N_{24}O_{18}$: calcd. C 19.24; H 2.49; N 29.92 %; found: C 19.13; H 2.42; N 29.86 %. **IR** (KBr): $\tilde{\nu}$ = 3138 w, 2853 s, 2360 s, 1655 s, 1565 v, 1511 v, 1393 s, 1310 w, 1181 m, 1103 m, 805 w, 699 m cm^{-1}.

Synthesis of $[Mn(tza)_2]_n$ (4): $Mn(CH_3COO)_2\cdot 4H_2O$ (0.0245g, 0.1 mmol) and Htza (0.0512 g, 0.4 mmol) were dissolved in a water/ethanol mixed solution (6 mL, v:v = 1:2). The mixture was stirred at room temperature for 1 h. Two months later, fleshcolor block crystals were obtained. Yield: 33 % (based on Htza). $MnO_4N_8C_6H_6$: calcd. C 23.29; H 1.94; N 36.23 %; found: C 23.16; H 1.90; N 36.19 %. **IR** (KBr): $\tilde{\nu}$ = 3164 s, 3029 w, 2948 w, 1628 s, 1488 w, 1432 m, 1399 s, 1319 m, 1268 m, 1179 s, 1103 s, 1001 m, 889 w, 69 9m, 579 w cm^{-1}.

Syntheses of $\{[Bi(tza)(C_2O_4)(H_2O)]\cdot H_2O\}_n$ (5) and $[Fe_3O(tza)_6(H_2O)_3]NO_3$ (6): Two energetic coordination compounds $\{[Bi(tza)(C_2O_4)(H_2O)]\cdot H_2O\}_n$ (**5**) and $[Fe_3O(tza)_6(H_2O)_3]NO_3$ (**6**) were synthesized by our research group via one-pot method in the previous work, and their structures have been described by *Kang* et al. in detail.[16] However, their catalytic effects on the thermal decomposition of HMX have not been studied yet.

Caution: Appropriate safety precautions should be taken.

Samples Preparation for the Catalytic Effect of Compounds 1–6 on the Thermal Decomposition of HMX: To check the catalytic effects of compounds **1–6** on the thermal decomposition of HMX, the compounds were mixed with HMX respectively at a mass ratio of 1:3, respectively, to prepare the test samples by grinding method.

Samples Preparation for the Synergetic Catalytic Effect on the Thermal Decomposition of HMX: In order to study the synergetic catalytic effect, mixtures of compound **1** and **2** at mass ratios of 3:1, 2:1, 1:1, 1:2 and 1:3 were prepared, which were named M_1, M_2, M_3, M_4, M_5, respectively. Mixtures of compounds **3** and **4** (M_6, M_7, M_8, M_9, M_{10}), **5** and **6** (M_{11}, M_{12}, M_{13}, M_{14}, M_{15}) were also prepared in the same way by grinding method to obtain them.

HMX mixtures consist of HMX and the mixtures of compounds **1** and **2**, **3** and **4** or **5** and **6** at a mass ratio of 3:1 (HMX to the mixtures of compounds). They were also obtained by grinding method.

Acknowledgements

This work was supported by the National Natural Science Foundation of China (No. 21371159, 21201155 and 120247–13).

Keywords: Tetrazole-1-acetic acid; Synergetic catalytic effect; HMX thermal decomposition

References

[1] K. Ramesh, S. N. Jawalkar, S. Sachdeva, Mehilal, B. Bhattacharya, *Cent. Eur. J. Energ. Mater.* **2012**, 49–58.
[2] B. Florczak, *Cent. Eur. J. Energ. Mater.* **2008**, 103–111.
[3] Y. Sun, B. Zhu, S. Li, *Def. Sci. J.* **2011**, *61*, 206–213.
[4] R. Dubey, P. Srivastava, I. P. S. Kapoor, G. Singh, *Thermochim. Acta* **2012**, *549*, 102–109.
[5] Q. L. Yan, F. Q. Zhao, K. K. Kuo, X.-H. Zhang, S. Zeman, L. T. DeLuca, *Prog. Energy Combust. Sci.* **2016**, *57*, 75–136.
[6] C. Wang, J. Li, X. Fan, F. Zhao,W. Zhang, G. Zhang, Z. Gao, *Eur. J. Inorg. Chem.* **2015**, *2015*, 1012–1021.
[7] J. Li, C. Wang, X. Gao, F. Zhao, K. Zhao, X. Fan, G. Zhang, W. Zhang, Z. Gao, *Polyhedron* **2016**, *106*, 58–64.
[8] X. Fan, C. Wang, J. Li, G. Zhang, *Z. Anorg. Allg. Chem.* **2015**, *641*, 1169–1175.
[9] Z. Cheng, G. Zhang, X. Fan, F. Bi, F. Zhao, W. Zhang, Z. Gao, *Inorg. Chim. Acta* **2014**, *421*, 191–199.
[10] E. Shao, D. Li, J. Li, G. Zhang, W. Zhang, Z. Gao, *Z. Anorg. Allg. Chem.* **2016**, *642*, 871–881.
[11] Q. Yang, J. Ge, Q. Gong, X. Song, J. Zhao, Q. Wei, G. Xie, S. Chen, S. Gao, *New J. Chem.* **2016**, *40*, 7779–7786.
[12] D. Jing, D. Chen, G. Fan, Q. Zhang, J. Xu, S. Gou, H. Li, F. Nie, *Cryst. Growth Des.* **2016**, *16*, 6849–6857.
[13] J. Han, J. Meeprasert, P. Maitarad, S. Nammuangruk, L. Shi, D. Zhang, *J. Phys. Chem. C* **2016**, *120*, 1523–1533.
[14] H. Ren, Y. Liu, Q. Jiao, X. Fu, T. Yang, *J. Phys. Chem. Solids* **2010**, *71*, 149–152.
[15] T. Wei, Y. Zhang, K. Xu, Z. Ren, H. Gao, F. Zhao, *RSC Adv.* **2015**, *5*, 70323–70328.
[16] L. Kang, Z. Wei, J. Song, Z. Yan, S. Meng, J. Xie, *RSC Adv.* **2016**, *6*, 33332–33338.
[17] Z. M. Li, G. T. Zhang, *Acta Chim. Sinica* **2011**, *69*, 1253–1258.
[18] S. Wang, L. Yang, T. Zhang, G. Zhang, J. Zhang, Z. Zhou, *J. Coord. Chem.* **2011**, *64*, 2583–2591.
[19] L. N. Li, University of Yunnan, China, **2010**.

[20] W. W. Dong, J. Zhao, L. Xu, *Cryst. Growth Des.* **2008**, *8*, 2882–2886.

[21] Q. Yu, X. Zhang, H. Bian, *Cryst. Growth Des.* **2008**, *8*, 1140–1146.

[22] C. S. Zhou, G. Fan, S. P. Chen, F. Q. Zhao, B. J. Jiao, S. L. Gao, *Acta Chim. Sinica* **2008**, *66*, 1776–1780.

[23] J. Wei, D. Zhang, Q. Yang, S. Chen, S. Gao, *Inorg. Chem. Commun.* **2013**, *30*, 13–16.

[24] P. B. Kulkarni, T. S. Reddy, J. K. Nair, A. N. Nazare, M. B. Talawar, T. Mukundan, S. N. Asthana, *J. Hazard. Mater.* **2005**, *123*, 54.

[25] O. Ordzhonikidze, A. Pivkina, Y. Frolov, N. Muravyev, K. Monogarov, *J. Therm. Anal. Calorim.* **2011**, *105*, 529–534.

[26] W. Pang, X. Fan, Y. Xue, H. Xu, W. Zhang, X. Zhang, Y. Li, Y. Li, X. Shi, *Propellants Explos. Pyrotech.* **2013**, *38*, 278–285.

[27] L. Ai, C. Zhang, L. Li, J. Jiang, *J. Appl. Catal. B Environ.* **2014**, *148*, 191–200.

Received: March 19, 2017

Z.-X. Wei, Y.-Y. Qu, L. Kang, F. Xie, H.-D. Zhang, P. Yue* **1–8**

Synergistic Catalytic Effect of a Series of Energetic Coordination Compounds based on Tetrazole-1-acetic Acid on Thermal Decomposition of HMX